Complex magnetic susceptibility setup for spectroscopy in the extremely low-frequency range

B. W. M. Kuipers,[a] I. A. Bakelaar, M. Klokkenburg, and B. H. Erné
Van't Hoff Laboratory for Physical and Colloid Chemistry, Science Faculty, Utrecht University, Padualaan 8, 3584 CH Utrecht, The Netherlands

(Received 7 September 2007; accepted 2 December 2007; published online 2 January 2008)

A sensitive balanced differential transformer was built to measure complex initial parallel magnetic susceptibility spectra in the 0.01–1000 Hz range. The alternating magnetic field can be chosen sufficiently weak that the magnetic structure of the samples is only slightly perturbed and the low frequencies make it possible to study the rotational dynamics of large magnetic colloidal particles or aggregates dispersed in a liquid. The distinguishing features of the setup are the novel multilayered cylindrical coils with a large sample volume and a large number of secondary turns (55 000) to measure induced voltages with a good signal-to-noise ratio, the use of a dual channel function generator to provide an ac current to the primary coils and an amplitude- and phase-adjusted compensation voltage to the dual phase differential lock-in amplifier, and the measurement of several vector quantities at each frequency. We present the electrical impedance characteristics of the coils, and we demonstrate the performance of the setup by measurement on magnetic colloidal dispersions covering a wide range of characteristic relaxation frequencies and magnetic susceptibilities, from $\chi \approx -10^{-5}$ for pure water to $\chi > 1$ for concentrated ferrofluids. [DOI: 10.1063/1.2827450]

I. INTRODUCTION

The dynamic magnetic properties of materials can be characterized by measuring the frequency-dependent magnetization in an alternating magnetic field. Here, a setup is presented that is designed to measure the complex magnetic susceptibility (a) at low frequencies, (b) on samples with a low magnetic susceptibility, and (c) using weak magnetic fields. These three specifications make the setup suitable to investigate colloidal dispersions of relatively large magnetic particles or aggregates ($\leqslant 1$ μm).

Previously, complex magnetic susceptibility spectra have mainly been measured to characterize the dynamic magnetic properties of ferrofluids,[1] but also to study the electrical conductivity of metals[2] and current vortices in superconductors.[3–6] With ferrofluids, which consist of concentrated colloidal dispersions of magnetic nanoparticles, the three mentioned specifications of the setup are not essential: (a) frequencies below 100 Hz generally correspond to the low-frequency limit because of the rapid dynamics of the nanoparticles,[1,7] (b) ferrofluids have a high magnetic susceptibility ($\chi > 1$),[1] and (c) fields below 1000 A/m are not expected to cause field-induced structures, because of the weak magnetic moment of the magnetic nanoparticles. For example, the interaction energy of iron oxide particles that are 10 nm in diameter with a field of 1000 A/m is less than 10% of the thermal energy k_BT. The situation is different for relatively large magnetic colloidal particles ($\leqslant 1$ μm): (a) they have much slower dynamics, (b) they can consist of composite material with a low volume fraction of magnetic material which leads to a low magnetic susceptibility, and (c) their dipole moment can nevertheless be much larger than that of magnetic nanoparticles, so that the interaction with a magnetic field can exceed the thermal energy already at weak fields below 1000 A/m.

Examples of large magnetic colloidal particles are composite magnetic microspheres,[8–10] magnetic paints,[11] elongated iron (hydr)oxide particles of hematite[12] or goethite,[13] and aggregates in destabilized ferrofluids.[14–19] For composite microspheres, measuring the complex magnetic susceptibility spectrum is a uniquely reliable way to determine the permanent magnetic dipole moment, since the frequency dependence indicates whether field-induced sample magnetization requires rotational motion of the microparticles.[8–10] For ferrofluids, measuring the complex magnetic susceptibility is a sensitive way to detect aggregation, since the time scale at which aggregates respond to an alternating magnetic field can be orders of magnitude longer than for single particles.[14–19] The complex magnetic susceptibility is also directly relevant for biomedical applications of magnetic nanoparticles.[20–24] For instance, cancer treatment by magnetic hyperthermia relies on the absorption of electromagnetic radiation, occurring at frequencies with an important loss signal or the so-called imaginary component of the complex magnetic susceptibility.[25–27]

One experimental approach to determine the complex magnetic susceptibility, in the time domain by magnetorelaxometry[28–33] or in the frequency domain,[34] would be to measure using a superconducting quantum interference device, with the possible disadvantage of requiring liquid helium infrastructure. However, our setup operates without cryogenics facility and realizes nevertheless suffi-

[a]Electronic mail: b.w.m.kuipers@uu.nl.

cient sensitivity with a balanced differential transformer optimized for work at low frequencies down to 0.01 Hz. Often, other ac susceptibility setups operate in the frequency range of >10 Hz (Refs. 35 and 36) or are dedicated to measurement at one frequency.[37] Generally, reversible magnetic susceptibility is a tensor with the reversible parallel susceptibility and two transverse susceptibilities as the diagonal elements.[38–40] In our setup the initial parallel magnetic susceptibility is measured.

In the next section, the setup and measurement procedure are presented, including the mathematics that relate the measured voltages to the complex magnetic susceptibility of the sample. In Sec. III, the new multilayered electromagnetic coils are characterized, and in Sec. IV, the performance of the setup is illustrated with measurements on magnetic colloidal dispersions. Finally, concluding remarks are given in Sec. V.

II. EXPERIMENTAL SETUP

A. General principle

The setup is based on a modified Hartshorn[41] bridge and consists of a balanced differential transformer. A single transformer would consist of two coils, with an alternating current applied to the primary coil and with the generated alternating magnetic field inducing an alternating voltage in the secondary coil. Since these coils are concentric, the parallel magnetic susceptibility is measured and because the bias (dc) field is zero, this is the initial susceptibility. The ratio between the output voltage and the input current is determined by the mutual inductance of the coils.[42–44] By comparing the output of two transformers, the difference is zero as long as both are identical, and it becomes nonzero when a magnetic sample is introduced that changes the mutual inductance of one of the two transformers. To obtain a strong signal with a weak magnetic field, we developed a new type of coils with a large sample volume, a great number of turns, and multiple primary and secondary layers. The sensitivity is then still limited by the fact that the two transformers are not exactly identical, leading to a background signal in the absence of a sample. We use a function generator to produce a compensation signal to cancel this remaining background.[45–47] In this way, the differential lock-in amplifier can operate at the highest sensitivity, not limited by the background signal but only by the sample signal and noise.

B. Hardware

Figure 1(a) schematically depicts the electronic equipment in the setup. Alternating voltages are produced by a Yokogawa FG120 dual channel function generator with a single synchronization reference. One output of the function generator (OSC1) is applied to the primary coils of the two transformers, which are connected in series so that the same current i flows through both. The signals of the secondary coils [sample (V_{sam}) and reference (V_{ref})] are subtracted from each other by an EG&G 5113 differential preamplifier (AMP1) with a software-controlled gain. The orientation of the coils is indicated with black dots. Using the second output of the function generator (OSC2), a compensation signal

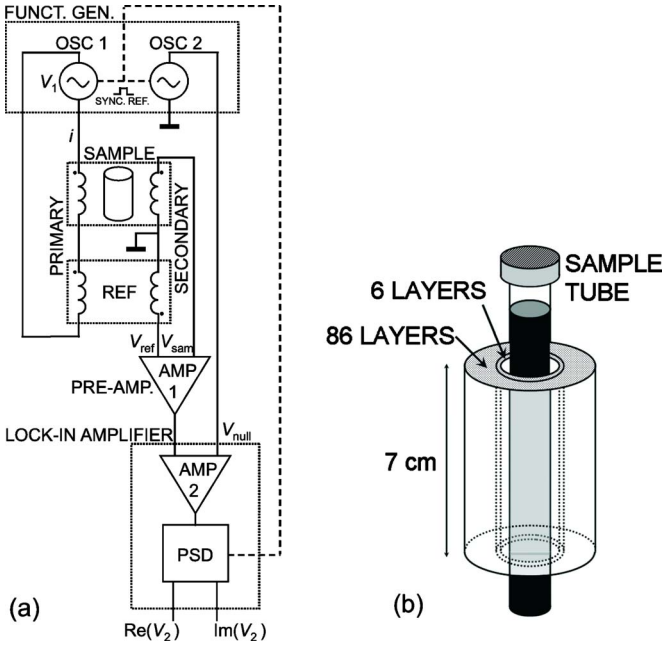

FIG. 1. (Color online) Schematic illustration of the setup with (a) the connections of the electronic equipment and (b) the multilayered sample transformer.

V_{null} can be generated that matches the output of the preamplifier, so that a minimal signal is measured at AMP2 of the 7265 Perkin Elmer dual phase DSP lock-in amplifier (0.001 Hz–250 kHz), whose gain is also software controlled. The phase-sensitive detector of the lock-in amplifier is synchronized to the function generator. The input voltage $V_1(\omega)$ is generated at OSC1 and the real (Re) and imaginary (Im) parts of the voltage $V_2(\omega)$ are the final output. The preamplifier (AMP1) can also be used in the single-ended input mode to measure the signal $V_{ref}(\omega)$ of the reference transformer; the measurement procedure (described later) ensures that this signal is the same in the presence and absence of a sample, so that the same current flows through the primary coils with and without the sample.

To shield from low-frequency magnetic interference, a grounded mu-metal inner box[48] is used ($35\times45\times20$ cm^3, 1.5 mm thick, attenuation factor=1000 for weak magnetic fields) from the MμShield Company (Goffstown, New Hampshire, U.S.A.). The mu-metal box is further shielded from electrical interference using a thermally insulated grounded Faraday cage (1 mm thick aluminum plates). Thermostatization is realized by circulating cooling liquid from a thermostatic bath (F40 Ultratemp 2000 from Julabo) through copper tubing surrounding the mu-metal box. A constant temperature is maintained at a Pt100 temperature probe placed inside the insulated box by feedback control.

The transformers were fabricated by Wikkelbedrijf Rijswijk (Driebruggen, the Netherlands) and consist of multiple concentric layers of enameled copper wire with a core diameter of 0.1 mm wound around a polyvinyl chloride cylinder with an external radius of 6.3 mm and an internal radius of 4.3 mm [total height of 7 cm, 636 turns per layer, see Fig. 1(b)]. The six inner layers constitute the primary coil (inner radius of 6.3 mm, outer radius of 7.0 mm) and the 86

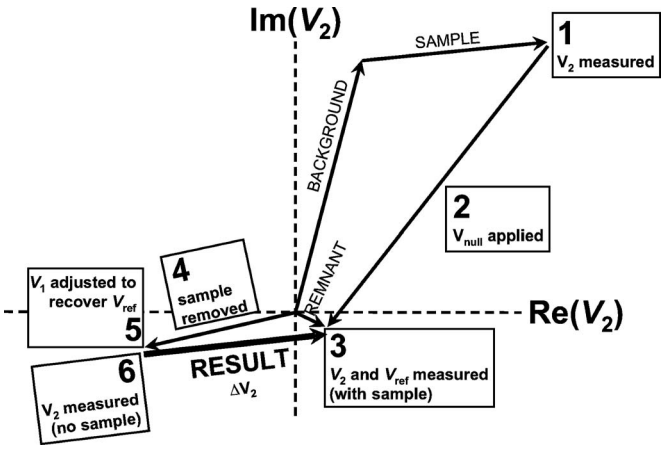

FIG. 2. Schematic illustration of the measurement sequence (see text and Fig. 1). The measurements are processed vectorially in the complex plane.

outer layers constitute the secondary coil (inner radius of 7.1 mm, outer radius of 18.2 mm). In principle, the dissipated power in the primary coil can be further reduced by choosing a larger copper wire core diameter. The layers are stacked such that a cross section would show a hexagonal stacking of the circular cross sections of the wires. Initially, the difference between the mutual inductances of the two transformers corresponded to 0.2% of that of a single one. To match the two even more closely, 80 extra turns were manually added to the transformer with the lowest mutual inductance, bringing the difference down to 0.05%. For further manual fine tuning down to a difference of about 0.01%, a small piece of ferrite was approached at a controlled distance from one of the transformers, thereby affecting its magnetic response.

Liquid samples are introduced inside the sample transformer using glass tubes with an external radius of at most 4.0 mm and an internal radius of at most 3.0 mm. The glass tubes are longer than the coils, so that they extend a few centimeters above and below the coils. In this way, sedimentation of a colloidal dispersion does not affect the measurements as long as the sedimentation front on top and the sediment at the bottom are about 1 cm outside the coil. The coils and the sample are held in position using Perspex® holders.

C. Measurement procedure

Different measurement procedures were implemented using LABVIEW software, and the most sensitive one is schematically depicted in Fig. 2. The initial output of the differential lock-in amplifier (step 1) corresponds to the difference between the sample and reference secondary coils. In step 2, the second output of the dual channel function generator (OSC2, see Fig. 1) is iteratively adjusted in such a way that V_{null} is practically equal to the output of the preamplifier (AMP1); the result of this "nullification" procedure is that the differential lock-in amplifier measures a remnant signal that is close to zero. In step 3, not only the remnant signal is measured but also the voltage $V_{ref}(\omega)$ of the secondary reference coil, by using the preamplifier in its single-ended input mode. This gives a measure of the current flowing through the primary coils. The removal of the sample is step 4. Removing the sample may significantly affect the total impedance of primary coils and therefore also the current flowing through them. Therefore in step 5, the first output of the function generator (OSC1) is iteratively adjusted until the signal $V_{ref}(\omega)$ measured by the secondary reference coil is again the same as in the presence of the sample; this ensures that current and external magnetic field are again the same as in the presence of the sample. Step 6 is the final measurement of the lock-in amplifier. The signal due to the sample can now be calculated by subtracting the remnant signal and inverting the sign. The result of this sequence of measurements is that the sample signal has been measured with the lock-in amplifier in its most sensitive possible range, not limited by the background signal but only by the sample signal and noise.

In the preferred sequence sketched in Fig. 2, the nullification in step 2 is carried out with the sample present followed by sample removal in step 4, instead of performing the nullification without sample and adding the sample in step 4. This has the following advantages. First, at each frequency, the gain of the preamplifier (AMP1) can be chosen the same with and without the sample (since removing the sample leads to a weaker signal), thereby avoiding possible artifacts resulting from comparing measurements performed at different gains. Second, when the maximum output voltage of the function generator is applied to the primary coils with the sample present, it remains possible to decrease the amplitude. This can be necessary because the impedance of the primary coils decreases upon removal of the sample, resulting in an increased current and magnetic field. If the maximum voltage were applied in the absence of the sample, it would no longer be possible to increase the amplitude of the applied voltage to compensate for the increased impedance of the coils upon addition of the sample. Third, removing rather than adding the sample halfway the measurement sequence shortens the time that is necessary to reestablish temperature equilibrium in the setup.

The amplitude of the voltage applied to the primary coils is limited at a default value of 2.5 V to avoid excessive heat dissipation. The secondary voltage is approximately linear with frequency, and with weakly magnetic samples it reaches 1 V at 100 Hz. This approaches the highest voltage that can be measured by the preamplifier AMP1. Therefore, above 100 Hz, the amplitude of the applied voltage is decreased linearly with frequency to keep the secondary voltage from exceeding 1 V. The amplitude of the applied voltage can also be chosen lower optionally. The software automatically decreases the amplitude if the presence of a highly magnetic sample causes a secondary voltage above 1 V. With a maximum current amplitude of 12.9 mA, a magnetic field of 730 A/m is reached.[49]

Depending on frequency, appropriate band filters are automatically chosen for the differential preamplifier and the lock-in amplifier. The time constants of both instruments can be chosen; for instance, it can be 1 s above 1 Hz and inversely proportional to frequency below 1 Hz. To vary the duration of the measurements, the operator can choose the number of iterations per frequency. With N iterations, each step in the measurement sequence (Fig. 2) is carried out N

times at each frequency before going to the next step. For $N>2$, the standard deviations in the real and imaginary components of the end result (the initial parallel magnetic susceptibility of the sample) are calculated on the basis of the standard deviations in the measurements of V_{ref} and V_2 with and without sample.

D. Calculation of the susceptibility

The alternating voltage $V_1(\omega)$ applied to the primary coils (see Fig. 1) generates an alternating current $i(\omega)$ according to their joint electrical impedance $Z_1(\omega)$,

$$i(\omega) = V_1(\omega)/Z_1(\omega), \tag{1}$$

where the sinusoidal alternating voltage is given by $V_1(\omega) = V_1^{\,0} \exp(j\omega t)$, with $V_1^{\,0}$ the amplitude of the applied voltage, j the square root of -1, $\omega=2\pi f$ the radial frequency, f the frequency in hertz, and t time in seconds. The alternating current in the primary coil generates an alternating magnetic field, which induces an alternating voltage in the secondary coils,

$$V_{\mathrm{ref}}(\omega) = -j\omega M i(\omega), \tag{2}$$

where M is the mutual inductance of the reference transformer, which is approximately equal to that of the sample transformer in the absence of a sample and approximately equals $\mu_0 n^2 z_1 z_2 \pi r^2/h$, where μ_0 is $4\pi\times10^{-7}$ J A^{-2} m^{-1}, n is the number of turns in one layer of the primary or secondary coils, z_1 and z_2 are the numbers of layers in the primary and the secondary coil, r is the root-mean-square radius of the primary coil, and h is the height of the cylindrical coils.

When a magnetic sample is inserted in the sample transformer, its mutual inductance is multiplied by a factor of $1+\chi(\omega)F$, where $\chi(\omega)$ is the dimensionless initial parallel magnetic susceptibility of the sample and F is the fill factor, which expresses to what extent that the central space inside the coils is filled by the sample. For a filled tube that spans the entire height of the coils, F is approximately equal to the internal cross section of the sample tube divided by the root-mean-square cross section πr^2 of the sample coil ($r\approx6.65$ mm). In terms of Fig. 1(a), this means that the complex susceptibility of the sample can be calculated from $\Delta V_2(\omega)$, defined as the difference between the final output voltages $V_2(\omega)$ with and without sample inside the coil, and from $V_{\mathrm{ref}}(\omega)$, the voltage generated by the reference transformer alone, which is proportional to the primary current i,

$$\chi(\omega)F = \Delta V_2(\omega)/V_{\mathrm{ref}}(\omega). \tag{3}$$

The phase of the complex quantity $V_{\mathrm{ref}}(\omega)$ is used as a reference to correct the phase information in $\Delta V_2(\omega)$ to obtain directly the real and imaginary components of $\chi(\omega)$.

III. CHARACTERIZATION OF THE COILS

Figure 3 presents electrical impedance spectra of a multilayered transformer, as described in Sec. II B, measured using an Autolab PGSTAT100 from EcoChemie (Utrecht, the Netherlands). Below 1 kHz, the impedance spectra of separate primary or secondary coils can be fitted excellently as a resistance R in series with an inductance L ($R=365\ \Omega$ and $L=0.036$ H for the primary coil, $R=9700\ \Omega$ and $L=18$ H for the secondary coil). Introducing a ferrofluid sample with a strong and frequency-independent magnetic susceptibility affects only the inductive component of the coil impedance (with a phase of +90°), by a frequency-independent factor; as a result, the lower the frequency is, the smaller the effect of the sample on the mainly resistive impedance [Fig. 3(c)]. By contrast, the mutual inductance of the primary and secondary coils only involves the inductive properties of the coils [Figs. 3(e) and 3(f)] and as a result, it is affected by the ferrofluid sample in a frequency-independent way [Fig. 3(g)]. This has a clear advantage compared to measuring on a single coil. Moreover, the impedance of a single coil has a much higher temperature dependence [compare Figs. 3(d) and 3(h)] because the resistivity of copper wires varies by about 0.4 % / °C. With our new setup, the mutual inductance of the coils was found to be 0.462 H, corresponding to the transfer function of order of 1 at 100 Hz in Fig. 3(e). Adding the ferrofluid sample increases the transfer function by about 40%, in agreement with the fill factor, $F=(3.0\ \mathrm{mm})^2/(6.6\ \mathrm{mm})^2=20.4\%$, and the susceptibility of the sample, $\chi\approx2$ (see Sec. II D).

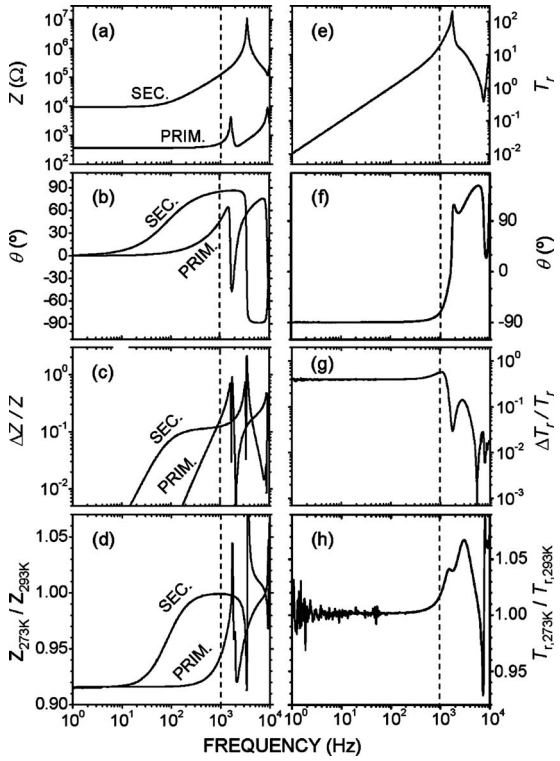

FIG. 3. (a)–(d) Electrical impedance spectra of a primary coil ("PRIM.") and a secondary coil ("SEC.") at 293 K: (a) magnitude, (b) phase, (c) relative change in magnitude due to a tube of ferrofluid filling the sample space (susceptibility $\chi\approx2$, internal radius: 3.0 mm), and (d) effect of cooling from 293 to 273 K. The transfer function $T_r=2V_{\mathrm{sec}}(\omega)/V_1(\omega)$ from one primary to one secondary coil is shown for comparison: (e) its magnitude, (f) its phase, (g) the effect of the ferrofluid sample, and (h) the effect of temperature.

Above 1000 Hz, the transformers can no longer be used to measure magnetic susceptibilities: the impedance spectra exhibit resonances and the effect of the ferrofluid sample decreases with increasing frequency, partly due to absorption of the alternating magnetic field by the copper wires and because of capacitive losses between neighboring wires.

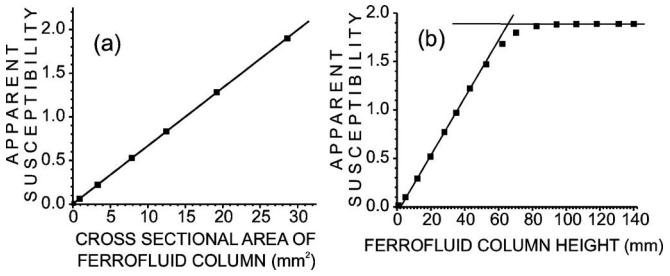

FIG. 4. Apparent susceptibility as a function of the amount of ferrofluid (with a susceptibility $\chi \approx 2$) in the sample space: (a) dependence on the cross-sectional surface area of the sample, and (b) dependence on the filling level of the sample tube, the center of the ferrofluid column being halfway the height of the coils.

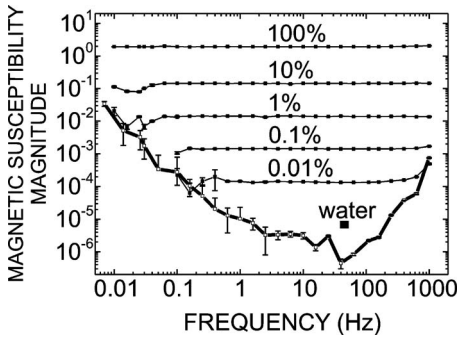

FIG. 5. Magnetic susceptibility for a dilution series of ferrofluids ranging from $\chi = 2 \times 10^{-4}$ to $\chi = 2$ (10 iterations per frequency, time constant of 1 s above 1 Hz, temperature=295.3 K). The thick line near the bottom indicates the background signal measured for an empty coil.

The spatial dependence of the magnetic field inside the sample area is illustrated in Fig. 4. First, measurements were done on tubes of different radii filled with ferrofluid. As expected, the signal from the sample scales with the cross-sectional area [Fig. 4(a)]. Second, measurements were performed as a function of the amount of ferrofluid contained inside a glass tube, with the ferrofluid centered at midheight of the transformer. The results in Fig. 4(b) indicate that the signal is not linear with the height of ferrofluid column at very low aspect ratios (column heights of a few millimeters) due to demagnetization.[50] The signal increases linearly as the height of the ferrofluid column goes from 10 to 50 mm. The signal no longer changes when the height of the ferrofluid column exceeds about 80 mm because the magnetic field rapidly decreases to zero above and below the 70 mm high coils. Analysis of Fig. 4(b) shows that the same signal would have been obtained for a 63 mm section of an infinitely long coil filled with this concentrated ferrofluid.

The absolute magnitude of the susceptibility was verified using a calibrated Kappabridge KLY-3 susceptibility meter from Agico, which operates at 875 Hz. The susceptibility of a diluted ferrofluid (diluted to minimize demagnetization effects) was found to be 0.0141 ± 0.0003 with the new setup presented here (taking into account the earlier mentioned fill factor of 20.4%), in agreement with 0.0138 ± 0.0001 found with the KLY-3 meter.

IV. SUSCEPTIBILITY SPECTRA

The wide susceptibility and frequency ranges of the setup are illustrated in Fig. 5. Measurements were carried out on a dilution series of ferrofluids whose magnetic susceptibility is frequency independent below 1000 Hz. The ferrofluids consisted of magnetite (Fe_3O_4) nanoparticles of about 7 nm in diameter[51,52] dispersed in a solution of 0.3 vol % oleic acid and 0.3 vol % oleylamine in Decalin.[53] As expected, frequency-independent magnitudes of the magnetic susceptibility were found, and in the 0.1–100 Hz range, an absolute phase smaller than 1° was measured, in line with the frequency independence of the magnetic susceptibility of the samples.

At low frequencies and low magnetic susceptibilities, the signal is limited by noise, as seen from the background signal that is inversely proportional to frequency. At frequencies that approach 1000 Hz, the background signal is due to a change in temperature of the coils by the alternating current. Since the sample and reference transformers are not exactly the same, the heating of the coils generates a differential signal, also because the measurements do not take exactly the same amount of time in the presence or absence of sample, leading to differences in the time available for heating and heat dissipation.

The sensitivity is the highest between 1 and 100 Hz (see Fig. 5), where it is possible to detect the diamagnetic susceptibility of simple solvents such as water ($\chi \approx -10^{-5}$), as is shown in Fig. 6. Although the measured magnitude is correct, the phase of the negative susceptibility gradually increases from close to 0° at 1 Hz to more than 90° at 100 Hz [Fig. 6(a)]. This is due to the coil heating artifact already discussed for Fig. 5. In principle, this artifact can be dimin-

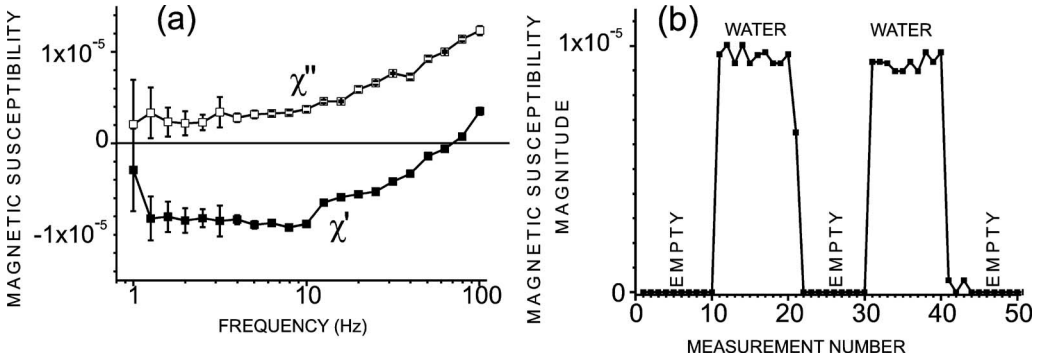

FIG. 6. Complex magnetic susceptibility measurements on water, (a) real (χ') and imaginary (χ'') components as a function of frequency and (b) magnitude as a function of time at 10 Hz using a glass sample tube that is alternatingly empty or filled with water (time constant: 10 s).

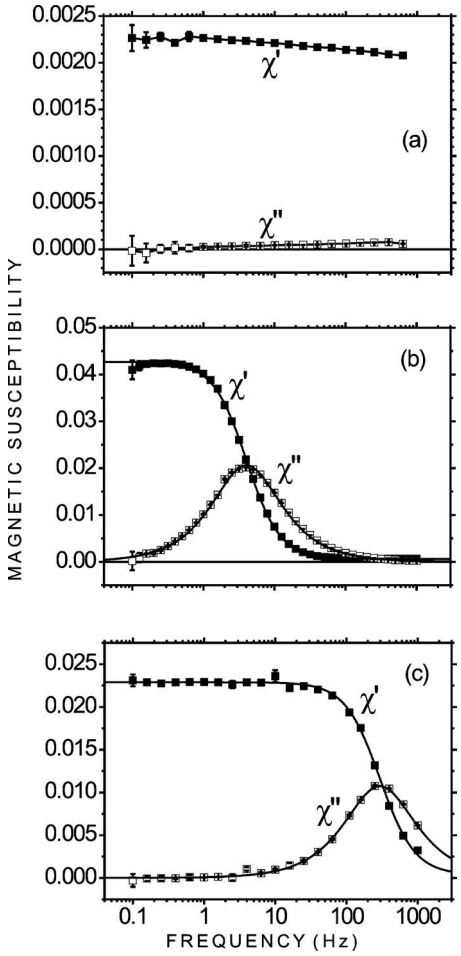

FIG. 7. Complex magnetic susceptibility spectra at 295.3 K of colloidal dispersions: (a) aqueous dispersion of superparamagnetic Dynabeads with a radius of 500 nm, (b), ethanolic dispersion of spherical silica particles with a radius of 228 nm and embedded cobalt ferrite nanoparticles, and (c) aqueous dispersion of spherical latex particles with a radius of 58 nm and embedded cobalt ferrite nanoparticles (Ref. 8).

ished by examining the effect of pumping water in and out of the sample tube. This procedure is used to demonstrate that the measured susceptibility clearly originates from the water sample [see Fig. 6(b)].

The intended purpose of the setup was to measure complex magnetic susceptibility spectra of liquid dispersions of relatively large colloidal particles. Figure 7 presents a number of such spectra, which can be described by the following equation:[1,16]

$$\chi = \chi_0 \omega_{\text{char}}/(\omega_{\text{char}} + j\omega) \equiv \chi' - j\chi'', \tag{4}$$

where χ is the magnetic susceptibility, χ_0 is the low-frequency limit, ω is the radial frequency, and ω_{char} is the characteristic frequency. The results are presented with separate curves for the real (in phase) component, $\chi' = \chi_0 {\omega_{\text{char}}}^2/({\omega_{\text{char}}}^2 + \omega^2)$, and the imaginary (out of phase) component, $\chi'' = \chi_0 \omega \omega_{\text{char}}/({\omega_{\text{char}}}^2 + \omega^2)$. At the characteristic frequency the real component has an inflection point and the imaginary component a maximum, this is above 1000 Hz in Fig. 7(a), at 4 Hz in Fig. 7(b), and at 295 Hz in Fig. 7(c). Physically, the characteristic frequency indicates how fast the average orientation of the magnetic dipoles in the sample

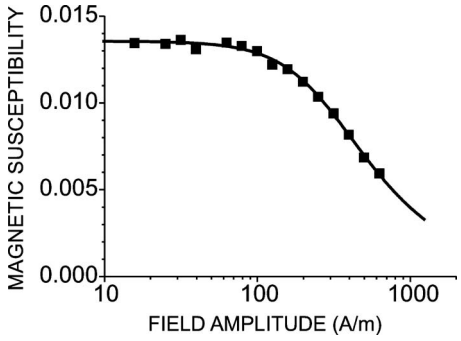

FIG. 8. Magnetic susceptibility at 1 Hz of a dispersion of silica particles (radius: 228 nm) with embedded cobalt ferrite as a function of the amplitude of the alternating magnetic field (Ref. 9).

reacts to a change in the external magnetic field. For the colloidal systems in Figs. 7(b) and 7(c), the characteristic frequency coincides with the rate of rotational diffusion of the spherical particles, given by $\omega_B = k_B T/[4\pi\eta(a_H)^3]$ where a_H is the hydrodynamic radius and η is the viscosity of the solvent. This means that a change in the magnetization of the entire sample requires rotation of the individual colloidal particles. This is unambiguous evidence that the colloidal particles have a permanent magnetic dipole moment.[8–10] By contrast, the particles of Fig. 7(a) have a magnetic relaxation that is much faster than the rate at which the particles rotate by thermal motion, indicating that those particles do not have a permanent magnetic dipole moment. In those microparticles, the embedded nanoparticles do have a permanent magnetic moment, but their dipolar orientation relaxes by Néel rotation inside the nanocrystal.[1,54,55]

The permanent magnetic dipole moment μ of the colloidal particles can be calculated from the low-frequency limit χ_0 of the magnetic susceptibility and the number concentration N/V of the particles: $\chi_0 = N\mu_0\mu^2/(3Vk_BT)$.[8–10] However, this assumes the weak field limit, meaning that the interaction of the dipoles with the magnetic field $\mu_0\mu H$ is negligible compared to the thermal energy k_BT. The permanent magnetic dipole moments of the colloidal particles in Figs. 7(b) and 7(c) are relatively large, so that the weak field limit is already exceeded at fields below 1000 A/m. This is illustrated in Fig. 8, where the low-frequency limit of χ is plotted versus the amplitude H of the alternating magnetic field. The analysis of such amplitude scans provides an alternative way to determine the magnetic dipole moment of the particles, with the advantage that the exact concentration does not have to be known.[9]

V. CONCLUSIONS

The described differential transformer is well suited for its intended purpose: to measure the magnetization dynamics of liquid dispersions of large colloidal particles ($\leqslant 1$ μm). The rotational dynamics of such particles correspond to characteristic frequencies within the 0.01–1000 Hz range. When magnetic relaxation occurs at the same frequency as Brownian rotational motion, this is unambiguous evidence that the particles have a permanent magnetic dipole moment. To measure at higher frequencies, it is possible to use the same electronics and software but then with coils whose electrical

impedance remains mainly inductive until much higher frequencies. Here, as a result of the large number of secondary coil layers and a phase-adjusted compensation voltage, the sensitivity is sufficiently high to measure low-frequency spectra of the large colloidal particles, even when weak fields of 1000 A/m or less must be used in order to remain in the weak-field limit.

ACKNOWLEDGMENTS

We thank Hans Heesen and his team of instrument makers for constructing the thermostatized box, Maria Claesson and Stefano Sacanna for providing magnetic colloidal particles, and the Debye Institute for financial support.

[1] P. C. Fannin, Adv. Chem. Phys. **104**, 181 (1998).
[2] Y. Kraftmakher, Am. J. Phys. **68**, 375 (2000).
[3] K. Senapati, S. Chakrabarty, L. K. Sahoo, and R. C. Budhani, Rev. Sci. Instrum. **75**, 141 (2004).
[4] L. K. Sahoo, S. Patnaik, R. C. Budhani, and W. L. Holstein, Phys. Rev. B **63**, 214501 (2001).
[5] M. S. Raven and M. Salim, Meas. Sci. Technol. **12**, 744 (2001).
[6] C. Y. Huang, Mater. Chem. Phys. **38**, 21 (1994).
[7] P. C. Fannin, B. K. P. Scaife, and S. W. Charles, J. Phys. D **28**, 2003 (1995).
[8] B. H. Erné, M. Claesson, S. Sacanna, M. Klokkenburg, E. Bakelaar, and B. W. M. Kuipers, J. Magn. Magn. Mater. **311**, 145 (2007).
[9] E. M. Claesson, B. H. Erné, I. A. Bakelaar, B. W. M. Kuipers, and A. P. Philipse, J. Phys.: Condens. Matter **19**, 36105 (2007).
[10] E. M. Claesson, B. H. Erné, and A. P. Philipse, J. Phys.: Condens. Matter **19**, 286102 (2007).
[11] V. T. Peikov and A. M. Lane, J. Colloid Interface Sci. **206**, 350 (1998).
[12] S. Sacanna, L. Rossi, B. W. M. Kuipers, and A. P. Philipse, Langmuir **22**, 1822 (2006).
[13] G. J. Vroege, D. M. E. Thies-Weesie, A. V. Petukhov, B. J. Lemaire, and P. Davidson, Adv. Mater. (Weinheim, Ger.) **18**, 2565 (2006).
[14] V. M. Buzmakov and A. F. Pshenichnikov, J. Colloid Interface Sci. **182**, 63 (1996).
[15] P. C. Fannin, A. T. Giannitsis, and S. W. Charles, Eur. Phys. J.: Appl. Phys. **12**, 93 (2000).
[16] B. H. Erné, K. Butter, B. W. M. Kuipers, and G. J. Vroege, Langmuir **19**, 8218 (2003).
[17] M. Klokkenburg and B. H. Erné, J. Magn. Magn. Mater. **306**, 85 (2006).
[18] K. Petersson, D. Ilver, C. Johansson, and A. Krozer, Anal. Chim. Acta **573–574**, 138 (2006).
[19] Y. Bao, A. B. Pakhomov, and K. M. Krishnan, J. Appl. Phys. **99**, 08H107 (2006).
[20] Q. A. Pankhurst, J. Connolly, S. K. Jones, and J. Dobson, J. Phys. D **36**, R167 (2003).
[21] S. H. Chung, A. Hoffmann, S. D. Bader, C. Liu, B. Kay, L. Makowski, and L. Chen, Appl. Phys. Lett. **85**, 2971 (2004).
[22] S. H. Chung, A. Hoffmann, K. Guslienko, S. D. Bader, C. Liu, B. Kay, L. Makowski, and L. Chen, J. Appl. Phys. **97**, 10R101 (2005).
[23] A. P. Astalan, F. Ahrentorp, C. Johansson, K. Larsson, and A. Krozer, Biosens. Bioelectron. **19**, 945 (2004).
[24] G. Fonnum, C. Johansson, A. Molteberg, S. Mørup, and E. Aksnes, J. Magn. Magn. Mater. **293**, 41 (2005).
[25] R. E. Rosensweig, J. Magn. Magn. Mater. **252**, 370 (2002).
[26] R. Hergt, R. Hiergeist, I. Hilger, W. A. Kaiser, Y. Lapatnikov, S. Margel, and U. Richter, J. Magn. Magn. Mater. **270**, 345 (2004).
[27] R. Hergt, R. Hiergeist, M. Zeisberger, G. Glöckl, W. Weitschies, L. P. Ramirez, I. Hilger, and W. A. Kaiser, J. Magn. Magn. Mater. **280**, 358 (2004).
[28] T. Jonsson, J. Mattsson, P. Nordblad, and P. Svedlindh, J. Magn. Magn. Mater. **168**, 269 (1997).
[29] A. J. Rondinone, A. C. S. Samia, and Z. J. Zhang, Appl. Phys. Lett. **76**, 3624 (2000).
[30] O. Petracic, X. Chen, S. Bedanta, W. Kleemann, S. Sahoo, S. Cardoso, and P. P. Freitas, J. Magn. Magn. Mater. **300**, 192 (2006).
[31] D. Eberbeck, F. Wiekhorst, U. Steinhoff, and L. Trahms, J. Phys.: Condens. Matter **18**, 2829 (2006).
[32] F. Ludwig, E. Heim, and M. Schilling, J. Appl. Phys. **101**, 113909 (2007).
[33] E. Romanus, M. Hückel, C. Groß, S. Prass, W. Weitschies, R. Bräuer, and P. Weber, J. Magn. Magn. Mater. **252**, 387 (2007).
[34] A. D. Hibbs, R. E. Sager, S. Kumar, J. E. McArthur, A. L. Singsaas, K. G. Jensen, M. A. Steindorf, T. A. Aukerman, and H. M. Schneider, Rev. Sci. Instrum. **65**, 2644 (1994).
[35] S. B. Slade, G. Kassabian, and A. E. Berkowitz, Rev. Sci. Instrum. **67**, 2871 (1996).
[36] R. R. de Souza and C. J. Magon, Rev. Sci. Instrum. **69**, 431 (1998).
[37] C. P. Bidinosti and W. N. Hardy, Rev. Sci. Instrum. **71**, 3816 (2000).
[38] A. Hoare, R. W. Chantrell, W. Schmitt, and A. Eiling, J. Phys. D **26**, 461 (1993).
[39] L. Pareti and G. Turilli, J. Appl. Phys. **61**, 5098 (1987).
[40] M. Barbic, Rev. Sci. Instrum. **75**, 5016 (2004).
[41] L. Hartshorn, J. Sci. Instrum. **2**, 145 (1925).
[42] C. M. Brodbeck, R. R. Bukrey, and J. T. Hoeksema, Rev. Sci. Instrum. **49**, 1279 (1978).
[43] A. F. Deutz, R. Hulstman, and F. J. Kranenburg, Rev. Sci. Instrum. **60**, 113 (1989).
[44] P. Laurent, A. M. Konn, J. L. Mattei, Ph. Talbot, and M. Le Floc'h, J. Magn. Magn. Mater. **122**, 164 (1993).
[45] D. B. Hall, J. M. Knop, S. M. Ayers, G. A. Klemme, and G. A. Schreiber, Rev. Sci. Instrum. **64**, 3328 (1993).
[46] A. Bajpai and A. Banerjee, Rev. Sci. Instrum. **68**, 4075 (1997).
[47] M. S. Raven and M. Salim, Meas. Sci. Technol. **12**, 744 (2001).
[48] A. F. P. van Putten, *Electronic Measurement Systems* (Prentice Hall, New York, 1988).
[49] P. C. Scholten, J. Magn. Magn. Mater. **149**, 57 (1995).
[50] D.-X. Chen, J. A. Brug, and R. B. Goldfard, IEEE Trans. Magn. **27**, 3601 (1991).
[51] D. Bica, Rom. Rep. Phys. **47**, 265 (1995).
[52] G. A. van Ewijk, G. J. Vroege, and B. W. M. Kuipers, Langmuir **18**, 382 (2002).
[53] M. Klokkenburg, J. Hilhorst, and B. H. Erné, Vib. Spectrosc. **43**, 243 (2007).
[54] B. Fischer, B. Huke, M. Lücke, and R. Hempelmann, J. Magn. Magn. Mater. **289**, 74 (2005).
[55] B. Fischer, J. Wagner, M. Schmitt, and R. Hempelmann, J. Phys.: Condens. Matter **17**, 7875 (2005).